Joint EPRI – 123HiMAT International Conference on
Advances in High Temperature Materials
October 21–24, 2019, Nagasaki, Japan
J. Shingledecker, M. Takeyama, editors
https://doi.org/10.31339/asm.cp.am-epri-2019p0001

"REACTIVE" MICROSTRUCTURE: THE KEY TO COST-EFFECTIVE, FATIGUE-RESISTANT HIGH-TEMPERATURE STRUCTURAL MATERIALS

Dr.-Ing. Bernd Kuhn
Dr. Jennifer Lopez Barrilao
Dr.-Ing. Torsten Fischer

Institute of Energy and Climate Research (IEK)
Microstructure and Properties of Materials (IEK-2)
Forschungszentrum Juelich GmbH, Juelich, Germany

ABSTRACT

Future, flexible thermal energy conversion systems require new, demand-optimized high-performance materials. In order to provide a basis for the targeted development of fatigue-resistant, cost-effective steel grades, the microstructural damage to materials and the failure of conventional and novel steels were investigated in thermo-mechanical fatigue and fatigue crack propagation experiments. Based on the results, improved, ferritic "HiperFer" (High performance Ferrite) steels were designed, produced and characterized. A brief description of the current state of development is given.

INTRODUCTION

The German “Energiewende” makes utilities, plant and material manufacturers face demanding challenges with regard to the development, operation and maintenance of highly flexible, regenerative (e.g. concentrating solar thermal, biomass, power-to-X) and conventional (fossil fueled w/wo linkage to thermal energy storage devices) thermal energy converters and storage systems. At present, the focus of development still is on process related issues, with development of new materials, suitable to meet future requirements, not playing a major role so far.
The knowledge of cyclic, microstructural damage and its effect on the failure mechanisms and potentially associated loss of lifetime of conventional heat resistant, structural materials has to be considered to be at least in need of improved. The development of new materials optimized for cyclic operation suffers from this shortcoming.
In the following, the mechanical behavior of ferritic-martensitic (P91, T92, MarBN) and ferritic steels [1] (HiperFer [2, 3]) in cyclic loading will be discussed in detail. Finally, the improved properties of HiperFer steels specially optimized for fatigue resistance are described.

EXPERIMENTAL

Materials

The chemical compositions of the ferritic, Laves phase strengthened steels and conventional ferritic-martensitic steels are given in Table 1. HiperFer trial steels were produced by vacuum

induction melting of high purity elements by the Institute of Ferrous Metallurgy (IEHK) of the Rheinisch Westfälisch Technische Hochschule Aachen, homogenized, forged and hot-rolled to a plate thickness of 16 mm.

Table 1: Chemical composition (wt.-%) of the ferritic trial alloys

Batch-ID:	C	N	Cr	Mn	Si	Nb	W	V	Al	Ni	Mo	B
HiperFer 17Cr2/3	<0.01	0.01	17.1	0.18	0.25	0.63	2.41	-	-	-	-	-
HiperFer 17Cr5	<0.01	0.01	17.2	0.20	0.27	0.99	3.70	-	-	-	-	-
P91	0.1	0.051	8.1	0.46	-	0.073	-	0.18	0.34	0.33	0.92	-
P92	0.16	0.051	8.96	0.46	0.04	0.069	1.84	0.2	0.007	0.06	0.47	0.001
						Nd					**Co**	
MarBN	0.09	0.009	8.97	0.48	0.25	0.03	3.0	0.2	0.01	0.09	3.0	0.011

HiperFer 17Cr2/3 is a comparatively low-alloyed base composition, which achieves creep strength values beyond T/P92 in the hot-rolled state or with appropriate precipitation heat treatment after recrystallization. The case hardening variant 17Cr5 has been improved in terms of mechanical strength by increased W and Nb contents, but above all, the ability to respond to cyclic deformation by increased precipitation hardening.
P91/92 specimens were taken from pipe sections of 160 / 352 mm outer diameter and 20/50 mm wall thickness. Austenitizing and tempering were executed at 1050/1065 °C // 0.5/2 h // air cooling and 750/770 °C // 1/2 h // air cooling. MarBN specimens were extracted from a 100 * 200 * 68 mm^3 slab, which was austenitized and tempered at 1120 °C / 1 h / air cooling + 700 °C / 2 h / air cooling + 700 °C / 4 h / air cooling.

Thermo-mechanical Fatigue Testing

Thermo-mechanical fatigue (TMF) experiments were carried out applying inductive sample heating, controlled by Type R loop thermocouples and high-temperature extensometers directly attached to the gauge lengths of cylindrical specimens (with a gauge length / diameter of 15 / 6.8 mm). All experiments (both “out-of-phase, OP” and “in-phase, IP”) were performed in total strain control in a temperature range from (2)50 to 650 ° C. Heating and cooling of the specimens was performed at heating / cooling rates of dT / dt = 10 Ks^{-1} to minimize creep at temperatures beyond 580 °C. For the same reason, no holding time was implemented at the hot end of the cycle. Below 200 °C, the cooling rate was limited due to the limited amount of cooling air. For this reason the cooling cycle took about 85 s (in the temperature range from 50 to 650 °C).

Fatigue crack propagation experiments

Fatigue crack propagation experiments were carried out at modified compact tension (CT) specimens with a geometry (width, W = 40 mm, thickness, B = 10 mm, initial notch depth, a_0 = 10 mm) in accordance with ASTM testing standard [4], utilizing a servo hydraulic testing machine. Both determination of the cyclic stress intensity factor ΔK and the cyclic crack growth rate (by a 7-point polynomial method) were accomplished according to ASTM regulation [4]. The experiments were carried out in laboratory air at 650 °C, applying an R-value of 0.1 and a testing frequency of 20 Hz. The direct current potential drop (PD) technique was used to continuously monitor crack length, employing linear calibration.

Creep Testing

Cylindrical standard specimens with a gauge length / diameter of 30 / 6.4 mm were crept in laboratory air in dead weight-loaded, lever arm type creep machines, equipped with 3-zone resistance furnaces and axially actuated extensometers, attached to the gauge lengths. Type S thermocouples were attached to the gauge lengths of the specimens to ensure a temperature accuracy of +/- 3 ° C.

Microstructural Characterization

For microstructural examination, the mechanical testing specimens were embedded in epoxy resin, ground and polished to a finish of 1 to 2 microns. Samples for the analysis of Laves phase precipitation in HiperFer steels were additionally etched at 1.5 V in 5 % H_2SO_4 to increase the particle / matrix contrast. Subsequently, a Zeiss Merlin field emission scanning electron microscope was utilized for high-resolution microstructure characterization and acquiring EBSD (electron backscatter diffraction) images for quantitative grain size and localized deformation analysis. The generated micrographs were analyzed applying the commercial software package AnalysisPro® with regard to grain size development.

RESULTS AND DISCUSSION

Microstructural evolution in thermo-mechanical fatigue loading: “Reactive” vs. passive microstructure

Figure 1a displays a schematic comparison of typical thermo-mechanical fatigue life curves of ferritic-martensitic steel and ferritic HiperFer steel (100 % out-of-phase). To take into account the difference in tolerance to damage (reflected by the change in slope of the fatigue curve in the "failure" range, cf. Figure 1a) of the materials, service life was determined from the intersection of linear approximations to the "stable" and the "failure" curve sections of the fatigue curves (cf. “ferritic” curve in Figure 1a). Ferritic-martensitic steel (like P91, Fig. 1c) exhibits high initial strain range due to initially high dislocation density. During the first ~ 1000 cycles, however, the recorded stress range drops by typically one third, before the material enters a quasi-stable plateau phase of slightly negative slope. Finally, FM steel reaches the failure phase, which is characterized by a comparatively steep drop in stress range. This final drop is less pronounced in case of ferritic HiperFer steel.

Like demonstrated at P91 (Figure 1c: “as-received” microstructure), this is caused by steadily progressing degradation of the martensite lath structure. Contrary to the known formation of a ferritic sub-grain structure with a grain size that approximates the former austenite grain size under creep load, thermo-mechanical fatigue loading (out-of-phase, T: 250 – 650 °C, 100 % strain obstruction) causes polygonization of the martensite lath structure. The result of this is formation of sub-grains in the size of the former martensite lath width (Figure 1c: clearly visible in the “failured” state). This phenomenon can best be quantified by the evolution of grain aspect ratio AR (ratio of grain length to grain width) of the martensite laths given in Figure 2a. Oblonged martensite laths of AR $\geq$ 3 ("as-recieved" in Figure 1c) disappear with increasing number of cycles in favor of smaller, globular sub-grains of AR $\rightarrow$ 1 ("3000 cycles", Fig. 2a). This is not limited to highly deformed areas around crack tips, where large plastic distortions exist. Even without a strain concentrating crack the entire gauge length displays microstructural degradation ("intact edge", cf. Figure 1c) beginning in the phase of stable stress range already.

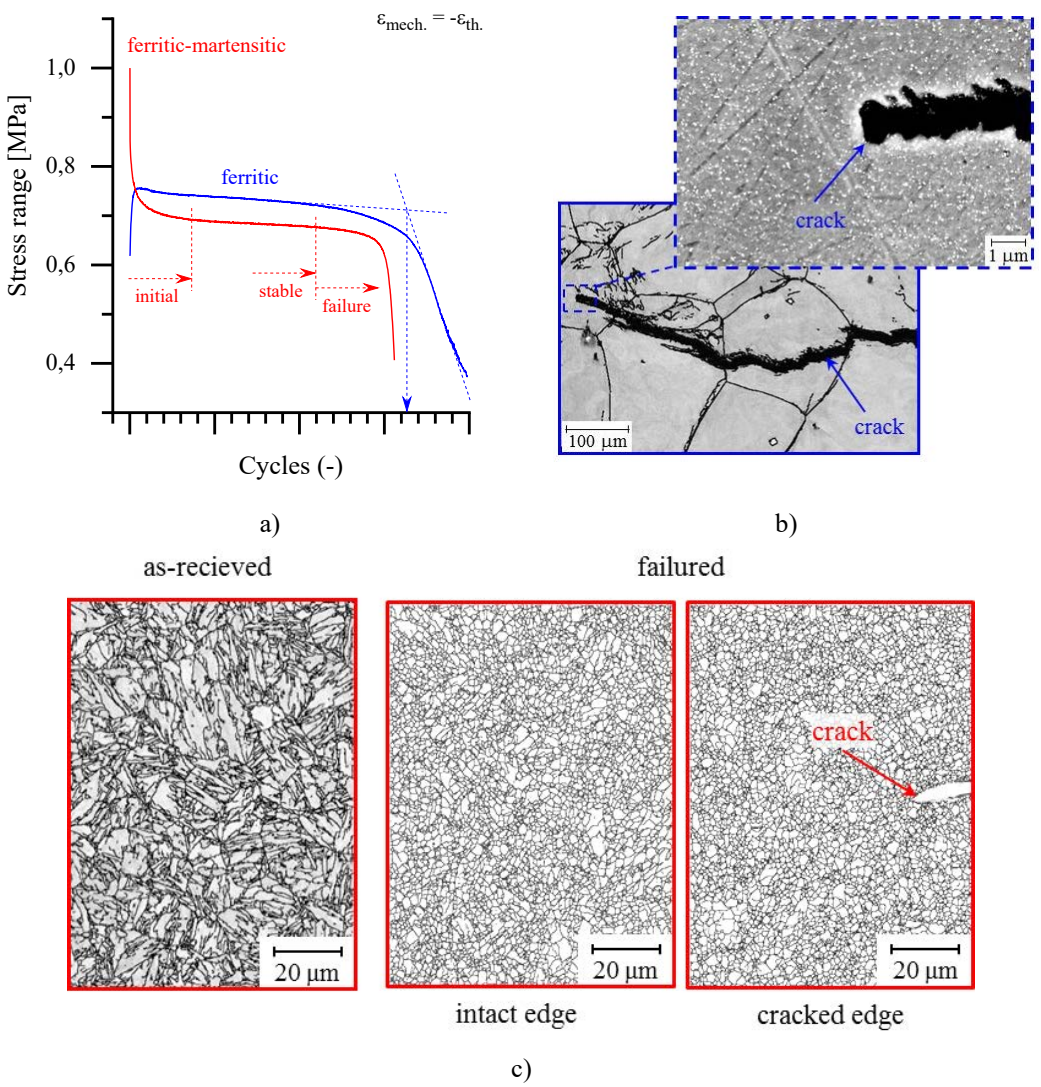

Figure 1: a) Typical thermo-mechanical fatigue curves of ferritic-martensitic steel and ferritic HiperFer steel. b) Stable grain structure and fine Laves phase particles in HiperFer and c) degradation of the martensite lath structure in ferritic-martensitic steel (P91). EBSD micrographs taken from out- of-phase tested TMF specimens, T: 250 – 650 °C, 100 % strain obstruction.

The main reason for the more forgiving character of HiperFer steel is thermo-mechanically induced precipitation of intermetallic Laves phase particles as a “reaction” to cyclic, plastic deformation at high temperature. HiperFer hardens during the initial, comparatively few cycles (by typically 30 %, cf. Figure 1a). In the damage phase, it exhibits reduced degression in stress range per cycle, resulting in prolonged TMF life. Caused by precipitation of fine Laves phase particles on grain boundaries, dislocations and sub-grain boundaries (both induced by cyclic deformation) the overall grain structure of this material type remains stable (Fig. 1b) for the entire lifetime. Recrystallization (i.e. sub-grain formation) is inhibited and thus restricted to narrow

areas in close vicinity of fatigue cracks. Crack progression is additionally hindered by precipitates concentrating in front of the crack tip, resulting in the outlined reduction of stress range degression per cycle (Figure 1a).

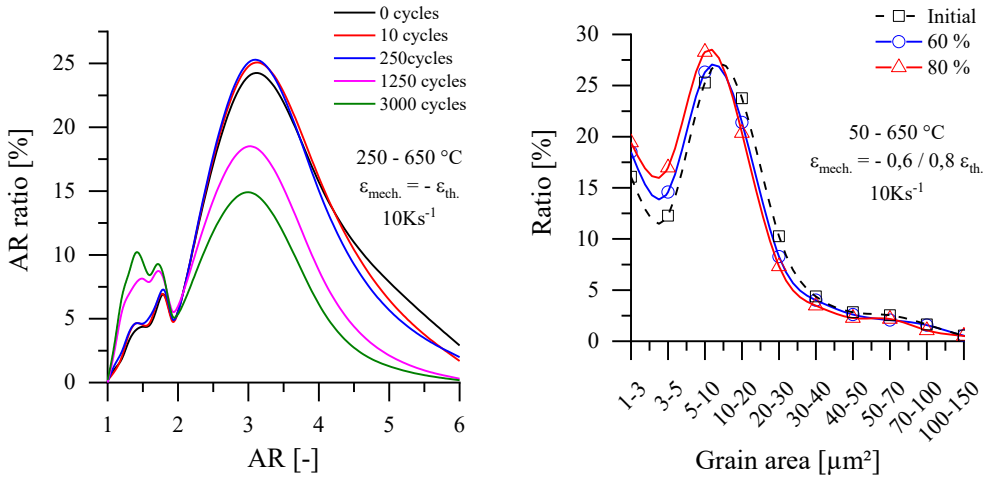

Figure 2: Evolution of a) aspect ratio AR of the martensite laths in P91 with increasing number of cycles (250 – 650 °C, out-of-phase, 100 % strain obstruction. Experiments terminated at given number of cycles, samples analyzed by EBSD and characterized by quantitative image analysis. For detection of sub-grain boundaries by EBSD a misorientation angle of 2° was defined.) and b) grain area distribution in P92 (50 – 650 °C, out-of-phase, 80 / 60 % strain obstruction; samples analyzed after failure, i.e. after 2715 / 5368 cycles in case of the 80 / 60 % experiment).

Sub-grain refinement also occurs in P92, but appears less homogeneous. Reduced (, more practice-relevant strain obstruction values of 80 % and 60 %) cause similar microstructural instability. In case of P92 (because of initially finer microstructure), the changes in sub-grain size become most apparent if the evolution of grain area distribution is utilized rather than aspect ratio AR. Figure 2b gives a comparison of the grain area distributions in the initial state and after out-of-phase TMF experiments with 60 / 80 % of thermal strain obstruction. With increasing strain obstruction a shift from grain areas larger than 10 µm^2 to smaller grain area can be observed. Similar microstructural changes have been reported under isothermal fatigue loading for polycrystalline copper [5], but also ferritic-martensitic steels like P91 [6] and P92 [7].

Nucleation and growth of short cracks: Thermo-mechanical fatigue life

The thermo-mechanical fatigue life of the characterized steels (ferritic-martensitic: P92, MarBN, ferritic: HiperFer 17Cr2/3 and 17Cr5) is comprehensively given in Figure 3. The higher stability of the grain structure, “reactive” hardening and crack inhibition result in improved resistance to thermo-mechanical fatigue of the ferritic, Laves phase strengthened HiperFer steels. In direct comparison to P92, 17Cr2/3 reaches almost doubled TMF lifetime over the entire span of stress (i. e. strain) ranges. In contrast, MarBN achieves about twice the number of loading cycles compared to 17Cr2/3. In the high-alloy version of HiperFer (17Cr5) precipitate formation, and thus an increase in strength, as a response to cyclic plasticization, has been maximized. In comparison to P92 up to 5.5 times longer technical fatigue life is obtainable over the entire stress range.

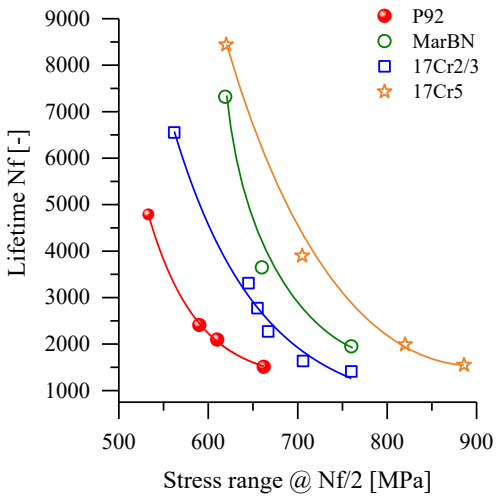

Figure 3: Thermo-mechanical fatigue life of ferritic and ferritic-martensitic steels over half-life stress range (50 - 650 °C, $\varepsilon_{mech.}$ = -0.6 $\varepsilon_{th.}$ to -1$\varepsilon_{th.}$, 10 Ks^{-1}, no holding times at $T_{min.}$ and $T_{max.}$)

Growth of long fatigue cracks: Residual life

Fatigue crack propagation of the tested steels in CT configuration is depicted in Figure 4a. Despite of much higher creep strength (cf. Fig. 6), and a slightly higher value of crack propagation initiation (Fig. 4a), stable crack propagation in MarBN almost resembles the behavior of P92.

Please note that the propagation initiation values given here were measured in crack propagation experiments (applying increasing ΔK values). For this reason they do not reflect true threshold values, which have to be recorded applying decreasing values of ΔK to exclude load sequence effects (e.g. increased residual dislocation strengthening from prior loading steps).

The ferritic HiperFer 17Cr2/3 alloy reaches stable crack propagation velocities, almost diminished by an order of magnitude. Based on thermo-mechanically induced precipitation hardening even constant crack propagation rate under increasing stress intensity is accessible, what poses superior residual life potential [11]. After testing micrographs were taken at two specific locations of the 17Cr2/3 CT specimen: The “annealed only” micrograph (Fig. 4b) was obtained from the heated part of the specimen, but in sufficient distance to the path of crack propagation to exclude an impact of cyclic deformation on the uniform distribution of fine Laves phase particles. The “fatigued” microstructure (Fig. 4b), taken in front of the crack tip, reflects the refining and boosting impact of cyclic plasticization on precipitation.

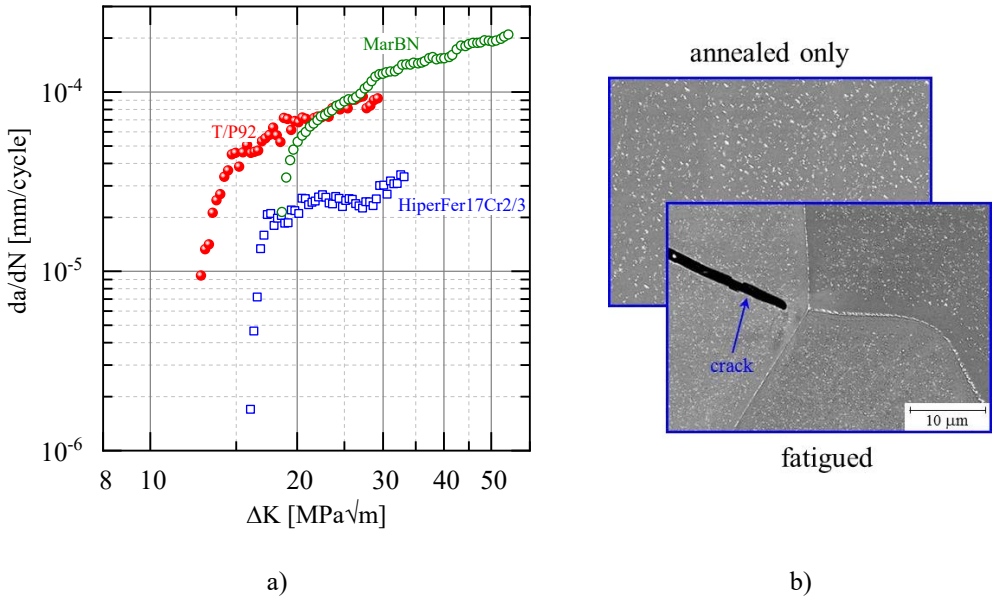

Figure 4: a) Fatigue crack propagation in ferritic-martensitic steels P92, MarBN and ferritic HiperFer 17Cr2/3 (650 °C, R = 0,1, f = 20 Hz). b) Refining impact of cyclic plasticization on Laves phase precipitation in 17Cr2/3.

Creep and creep / fatigue interaction

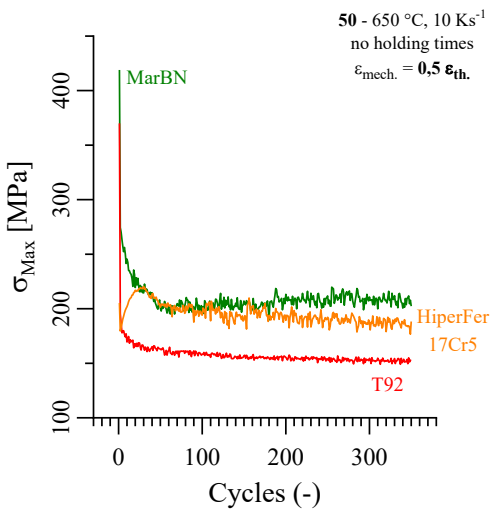

Figure 5: Maximum stress vs. cycle number plots from thermo-mechanical pre-fatiguing of T92, MarBN and HiperFer 17Cr5 (in-phase, 50 – 650 °C, 50 % of additional mechanical strain)

The microstructural degradation of ferritic-martensitic steels in thermo-mechanical fatigue loading discussed above suggests negative consequences for creep resistance in intermitting service, i.e. creep / fatigue interaction. For this reason, creep tests on thermo-mechanically pre-fatigued specimens (TFC) were performed.

Differing from the thermo-mechanical fatigue experiments, thermo-mechanical pre-loading was performed in in-phase experiments (thermal and mechanical expansion into the same direction) and in a cold-start simulating temperature interval from 50 to 650 °C. By this method of pre-fatiguing tensile stress (analogous to subsequent creep testing) is applied at the hot end of the TMF cycle (i. e. at 650 °C, the subsequent creep temperature) and a comparatively low level of additional mechanical strain (50 % of thermal strain) was selected. TMF pre-fatiguing was performed into the stable range of the resulting fatigue curves (Fig. 5), was then terminated and the samples subjected to creep subsequently.

Although MarBN and HiperFer 17Cr5 exhibit contrarian behavior in the initial phase of TMF pre-loading (Fig. 5: Recovery in case of MarBN, strengthening in case of 17Cr5) both reach a tensile stress level of appr. 180 MPa at the beginning of the stable stress range phase. At the hot end of the TMF cycle (650 °C) both reach almost similar tensile stress values (MarBN: 202 MPa; 17Cr5: 188 MPa). For this reason, a similar creep stress of 180 MPa was selected for the subsequent creep experiments on MarBN and 17Cr5. P92 reaches a lower tensile stress of about 150 MPa after 350 cycles. Due to the comparably low creep strength of P92 a reduced stress level of 100 MPa was selected rather than 150 MPa to ensure true creep behavior in the subsequent creep experiment. The creep lives of the thermo-mechanically pre-fatigued (TFC) materials are included in the stress rupture diagram in Figure 6.

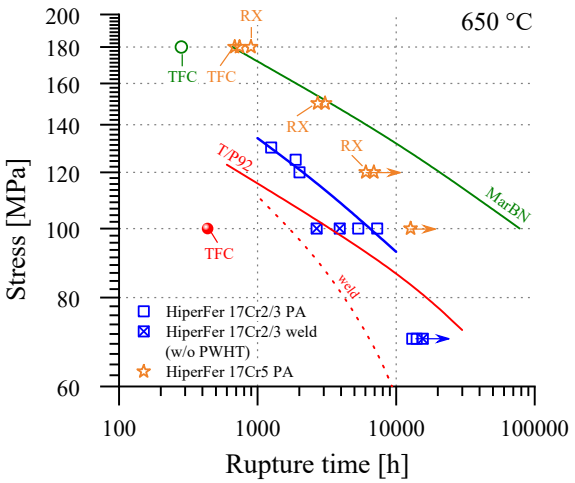

Figure 6: Creep strength with (TFC: thermo-mechanical fatigue / creep) / without thermo-mechanical pre-loading. HiperFer 17Cr2/3 was applied in precipitation annealed (PA) state only, 17Cr5 in PA and RX (recrystallized) condition. Creep tests in the pre-fatigued state were carried out at 100 / 180 MPa on T92 / MarBN and HiperFer 17Cr5 (comparative creep strength data: T/P92 [8], MarBN [9, 10]).

Figure 6 compares the creep strength of the ferritic HiperFer steels to T/P92 [8] and MarBN [9, 10]. The low-alloyed base material variant 17Cr2/3 surpasses T/P92. While creep deformation of intermetallic particle strengthened ferritic steels is mainly controlled by coarsening of the strengthening Laves phase precipitates [1, 12, 13, 14], creep damage and failure are mainly

related to the formation of particle free zones along high angle grain boundaries [14, 15]. The first welded joints (without post-weld heat treatment), produced with chemically matching filler metal, reach approximately the T/P92 base metal values at a creep stress of 100 MPa. With more than 15.500 h the welds have already reached more than twice the lifetime of T/P92 welds at a testing stress of 70 MPa. All the 70 MPa creep experiments at 17Cr2/3 and its welded joints are still in progress.

The results obtained so far on the high-alloy variant 17Cr5 suggest a high-stress creep strength (180, 150 MPa) close to MarBN. It is noteworthy that there is little difference in rupture time between the recrystallized (RX) and precipitation annealed (PA) states, what in turn means that 17Cr5 can be applied like austenitic, case hardening steel. All experiments below a stress of 150 MPa are still in progress.

In case of P92 TMF pre-loading leads to a reduction in creep life by almost 90 % at a stress of 100 MPa (from ~ 3300 h [8] to 436 h). For MarBN, however, TMF fatiguing causes a smaller decrease in creep life of about 60 % at a stress of 180 MPa (from ~ 660 h [9, 10] to 282 h). On the other hand, HiperFer 17Cr5 demonstrates a decrease of less than 20 % (from 819.5 h, the average of 897 h (RX) + 742 h (PA) to 685 h) at similar stress. While the creep rupture time after thermo-mechanical pre-loading of the HiperFer 17Cr5 material is within a $^{+}/_{-}$ 10 % scatter band, both ferritic-martensitic steels range far below.

Conclusion and outlook

P91 and P92 exhibit microstructural instability in thermo-mechanical fatigue loading with polygonization of the original martensite lath structure, limiting their fatigue, but especially creep life after thermo-mechanical pre-fatiguing. The same limitation appears in case of the maximum creep strength ferritic-martensitic steel MarBN, but to lesser extent.

The high-alloy, case-hardening variant of the stainless, ferritic HiperFer steels (17Cr5) achieves about the creep resistance of MarBN (on the basis of limited data available so far). HiperFer is tuned to react by thermo-mechanically induced formation of intermetallic precipitates of the Laves phase, when cyclically deformed at high temperature. For this reason, it provides a stable microstructure even under the most demanding operating conditions and combines excellent fatigue life, hardly diminished creep strength after previous thermo-mechanical fatiguing with superior resistance to steam oxidation and downtime corrosion.

Current work focuses on broadening the database with regard to creep resistance after pre-fatiguing and detailed microstructural analysis. In the medium term, the experimental program will be expanded to the role of thermo-mechanically induced crack branching on retardation of long fatigue cracks to derive suitable models for prediction of residual component life.

ACKNOWLEDGMENTS

The authors would like to express their gratitude for the supply of MarBN material by Siemens AG, financing of part of the work by the German Federal Ministry of Education and Research (FKZ: 03EK3032) and production of the HiperFer 17Cr2/3 welded joints by the Oak Ridge National Laboratory, Materials Science and Technology Division, USA.

REFERENCES

[1] Kuhn, B.; Talik, M.; et al, „Development of high chromium ferritic steels strengthened by intermetallic phases“, Materials Science & Engineering A 594 (2014) 372–380

[2] Kuhn, B.; Lopez Barrilao, J.; Singheiser, L.; Yamamoto, Y., “Development Status of High performance Ferritic (HiperFer) Steels”, Proc 8th International Conference on Advances in Materials Technology for Fossil Power Plants, October 11 – 14, 2016, Albufeira, Algarve, Portugal

[3] Kuhn, B., Talik, M., Lopez Barrilao, J., Singheiser, L., „Ferritische Hochleistungsstähle (HiperFer)–Ein Entwicklungsstatus“, 38. Vortragsveranstaltung der Forschungsvereinigung Warmfeste Stähle und Hochtemperaturwerkstoffe (FVWHT) 2015

[4] ASTM Standard E647 – 11

[5] Peralta, P., Laird, C., “Cyclic Plasticity and Dislocation Structures”, Reference Module in Materials Science and Materials Engineering, Elsevier (Amsterdam 2015), https://doi.org/10.1016/B978-0-12-803581-8.02917-9

[6] Nagesha, A., Kannan, R., Sandhya, R., Sastry, G. V. S., Mathew, M. D., Rao, K. B. S., Singh, V. S, “Thermomechanical Fatigue Behaviour of a Modified 9Cr-1Mo Ferritic-martensitic Steel”, Procedia Engineering 55 (2013), pp. 199 – 203

[7] Zhang, W., Wang, X., Lia, X., Gong, J., Wahab, M. A., “Influence of prior low cycle fatigue on microstructure evolution and subsequent creep behavior”, International Journal of Fatigue 109 (2018), pp. 114 – 125

[8] ECCC Datasheets 2014, ASTM Grade 92

[9] Abstoss, K. G., Nitsche, A., Mayr, P., Schlacher, C. , Gonzales, V., Aguero, A., “Experience with 9Cr3W3CoVNbBN steel in terms of welding, creep and oxidation”, Proc 8th International Conference on Advances in Materials Technology for Fossil Power Plants, October 11 – 14, 2016, Albufeira, Algarve, Portugal

[10] Hamaguchi, T., Okada, H., Semba, H., Hirata, H., Iseda, A., Yoshizawa, M., “Development of High Strength 9Cr-3W-3Co-Nd-B Heat Resistant Steel Tube and Pipe”, Proc 1st Conference on Advanced High-Temperature Materials Technology for Sustainable and Reliable Power Engineering, June 29 – July 03, 2015, Sapporo, Japan

[11] Schulz, A., Fischer, T., Beckert, M., Kuhn, B., Trieglaff, R., „Potentials and Issues of Additively Manufactured Components for Nuclear Power Plants”, Proc 25th SMiRT Conference, August 4 - August 9, 2019, Charlotte, North Carolina, USA

[12] Lopez Barrilao, J.; Kuhn, B.; Wessel, E.; Talík, M., “Microstructure of intermetallic particle strengthened high-chromium fully ferritic steels”, Materials Science and Technology, 33:9, 1056-1064, DOI: 10.1080/02670836.2016.1244039

[13] Lopez Barrilao, J.; Kuhn, B.; Wessel, E., „Identification, size classification and evolution of Laves phase precipitates in high chromium, fully ferritic steels“, Micron 101 (2017) 221–231; http://dx.doi.org/10.1016/j.micron.2017.07.010

[14] Lopez Barrilao, J.; Kuhn, B.; Wessel, E., „Microstructure evolution and dislocation behaviour in high chromium, fully ferritic steels strengthened by intermetallic Laves phases”, Micron 108 (2018) 11–18; https://doi.org/10.1016/j.micron.2018.02.008

[15] Kuhn, B.; Asensio Jimenez, C.; Niewolak, L.; Hüttel, T.; Beck, T.; Hattendorf, H.; Singheiser, L.; Quadakkers, W.J., „Effect of Laves phase strengthening on the mechanical properties of high Cr ferritic steels for solid oxide fuel cell interconnect application“, Materials Science and Engineering A 528 (2011) 5888–5899; doi:10.1016/j.msea.2011.03.112